

123. Preparation and ESR-Spectroscopical Investigation of Remarkably Persistent Oxoisobenzofuranyl Radicals

by Gary Kruppa¹⁾, Paul Hug, André Liégard, and Guenther Rist

Ciba, Physics Department, CH-4002 Basel

and Petr Nesvadba*

Ciba, Research Centre, CH-1723 Marly

(26. II. 93)

The synthesis of the diastereoisomeric 1,1'-diaryl-1,1'-bi(isobenzofuran)-3,3'(1*H*,1'*H*)-diones **3a-d** starting from the readily available 2-aryylbenzoic acids **1a-d** is described (*Scheme 1*). Of the colourless dimers **3a-d**, only the sterically congested **3a** and **3b** dissociate at ambient temperature in solution to the deep red free 3-oxoisobenzofuran-1-yl radicals **4a** and **4b**, respectively. The radicals **4a, b** are extremely persistent in the absence of O₂. The structures of these radicals are confirmed and the coupling constants assigned by ESR and ENDOR spectroscopy and computer simulation of their ESR spectra. The dissociation equilibrium constant at 20° in toluene for **3a** is determined to be $1.18 \cdot 10^{-5}$ M. By studying the steady-state radical concentration as a function of temperature, the enthalpy and entropy changes for the homolytic dissociation of **3a** are determined.

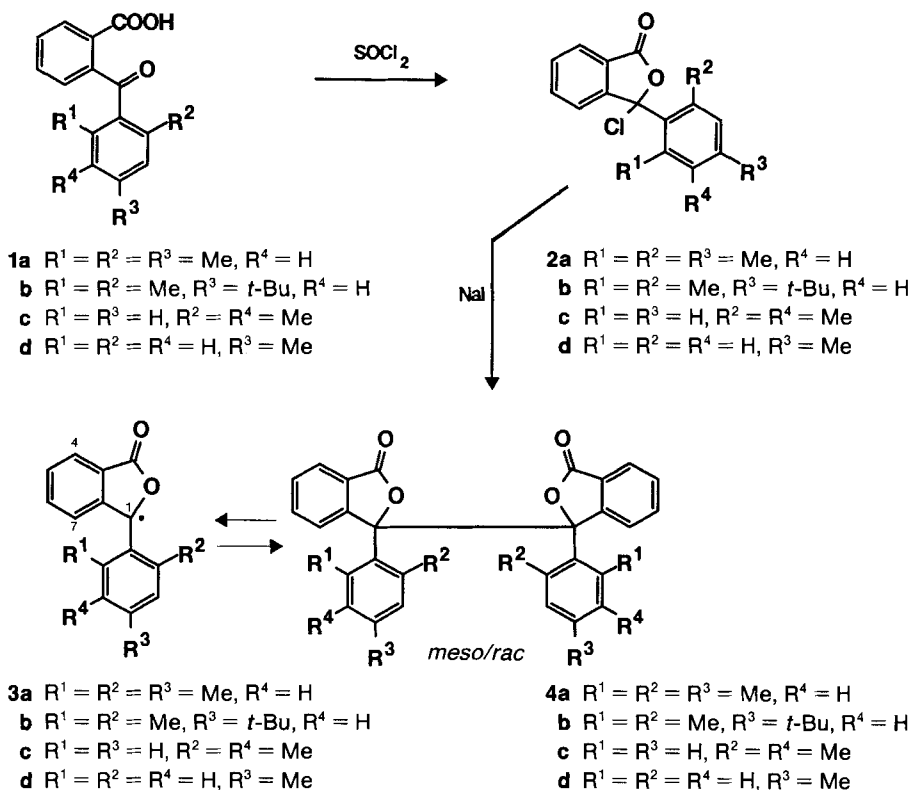
Introduction. – Diastereoisomeric *meso*- and *rac*-1,1'-diaryl-1,1'-bi(isobenzofuran)-3,3'(1*H*,1'*H*)-diones of type **3** can be prepared by the action of a variety of reducing agents [1] on 2-aryylbenzoic acids. Another method for their synthesis is the action of alkali iodide on 3-aryl-3-chloroisobenzofuran-1(3*H*)-ones as shown by *Bhatt et al.* [2] in 1971. A mechanism for this dimerisation which involves the formation of the intermediate oxoisobenzofuranyl radicals was postulated by the same authors, based on a subsequent kinetics study [3]; the presence of free radicals in this reaction was proven by trapping them as adducts with acrylonitrile. Free oxoisobenzofuranyl radicals were also proposed as intermediates in the photolysis of tertiary 2-benzoylbenzamides [4] which afforded 1,1'-diaryl-1,1'-bi(isobenzofuran)-3,3'(1*H*,1'*H*)-diones **3**. The reversible *thermal* homolytic cleavage of 1,1'-diaryl-1,1'-bi(isobenzofuran)-3,3'(1*H*,1'*H*)-diones into oxoisobenzofuranyl radicals would, on the other hand, explain the well known [5] thermal interconversion of their pure diastereoisomers during their recrystallisation from higher-boiling solvents.

We now report the preparation of the sterically highly strained 1,1'-diaryl-1,1'-bi(isobenzofuran)-3,3'(1*H*,1'*H*)-diones **3a** and **3b** and the ESR spectroscopic investigation of remarkably persistent oxoisobenzofuranyl radicals **4a, b** which in solution are in equilibrium with the former, even at room temperature.

Results. – 1. *Synthesis and Properties of 3a-d.* The 1,1'-diaryl-1,1'-bi(isobenzofuran)-3,3'(1*H*,1'*H*)-diones **3a-d** were prepared from the readily available 2-aryylbenzoic acids

¹⁾ Current address: *Bruker Instruments Inc.*, Manning Park, Billerica, MA 011828, USA.

Scheme 1



1a–d via **2a–d** using the method of *Bhatt et al.* [2] (see *Scheme 1* and *Exper. Part*). They are colourless solids and stable at room temperature under inert-gas atmosphere.

Bhatt's method is known to give **3** as 1:1 diastereoisomer mixtures (*meso*-**3**/*rac*-**3**). We were interested, in another context, however, in the pure diastereoisomers. The 1,1'-diaryl-1,1'-bi(isobenzofuran)-3,3'-(1*H*,1'*H*)-diones **3** with 2,6-unsubstituted aryl groups ($R^1 = R^2 = \text{H}$) are known [5] to be sufficiently thermally stable to allow separation of their diastereoisomer mixtures by chromatography or careful crystallisation from low-boiling solvents. Attempts to crystallise the pure *meso*- and *rac*-**3** from higher-boiling solvents like xylene, however, led to their partial interconversion. We separated the mixture **3c** into the higher- and lower-melting diastereoisomer on a preparative scale; however, no attempt to assign the configurations was made. The analytical baseline separation of mixture **3d** was also possible by reversed-phase HPLC. On the contrary, the dimers **3a, b**, which we assume to be also 1:1 diastereoisomer mixtures, were not separable by crystallisation or normal chromatographical techniques.

Surprisingly, the dimers **3a, b**, when dissolved in previously degassed solvents, dissociated to give already at room temperature deep-red solutions of radicals **4a, b** (see *Scheme 1*) which are extremely stable in the absence of O_2 . The red colour disappeared rapidly,

however, if air was admitted, or if the temperature was lowered sufficiently (to *ca.* -60°) so that all radicals **4a**, **b** were present as their dimers **3a**, **b**. Thus, the red solutions of the partially dissociated dimers **3a**, **b** in deoxygenated CDCl_3 at room temperature gave well resolved $^1\text{H-NMR}$ spectra after cooling to -60° (see *Exper. Part*). Interestingly, only one diastereoisomer could be seen in these low-temperature spectra. Hence, it seems, that only one diastereoisomer was formed in the recombination reaction at low temperature. The cleavage of dimer **3c** to afford the ESR-detectable concentration of radicals **4c** took place only at much higher temperature (see *Chapt. 3*). In the case of dimer **3d**, we were not able to reach the dissociation temperature.

2. *ESR Spectra and Coupling Constants.* The coupling constants obtained from the ENDOR spectra of the radicals **4a**, **b** are summarised in *Table 1*. The remaining coupling

Table 1. ENDOR Coupling Constants^{a)}

| Radical | Solvent | Temperature [K] | Coupling constant [G] ^{b)} | | | | | |
|-----------|---------------------|-----------------|-------------------------------------|-------|------|------|------|------|
| | | | 1 | 2 | 3 | 4 | 5 | 6 |
| 4a | toluene | 245 | 0.74 | 0.97 | 1.07 | 1.16 | 3.42 | 4.19 |
| | 2-chloronaphthalene | 298 | 0.73 | 0.96 | 1.11 | | 3.41 | 4.20 |
| | EtOH | 273 | 0.70 | 0.96 | 1.09 | | 3.45 | 4.14 |
| 4b | toluene | 253 | 0.71 | 0.045 | 1.03 | | 3.43 | 4.20 |

^{a)} Some of the hyperfine couplings not resolved. ^{b)} ± 0.02 G.

constant of **4a** was obtained from an analysis of the ESR spectra. At low radical concentration (in very dilute solutions of dimer or in more concentrated solutions at low temperature), an almost fully resolved ESR spectrum of **4a** could be obtained in toluene, 2-chloronaphthalene, or chloroform (see *Fig. 1* for a toluene solution at -25°). In *Fig. 2a*, an expanded plot of the first half of this ESR spectrum is reproduced, and in *Fig. 2b* the

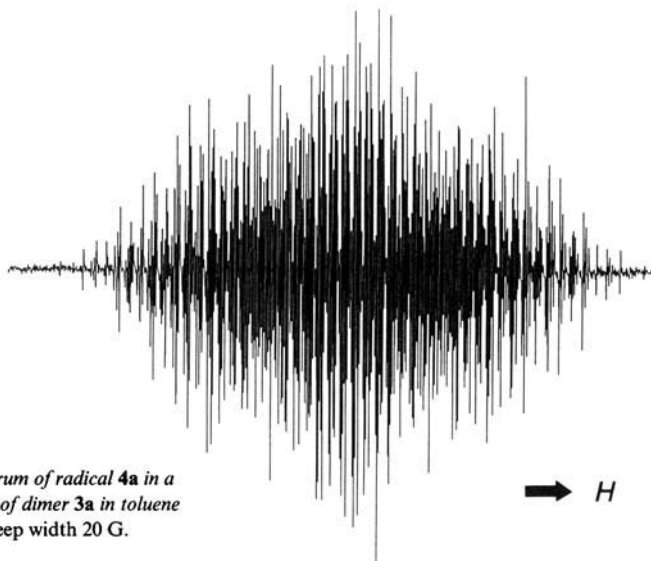


Fig. 1. ESR Spectrum of radical 4a in a $2 \cdot 10^{-3}$ M solution of dimer 3a in toluene at -25° . Total sweep width 20 G.

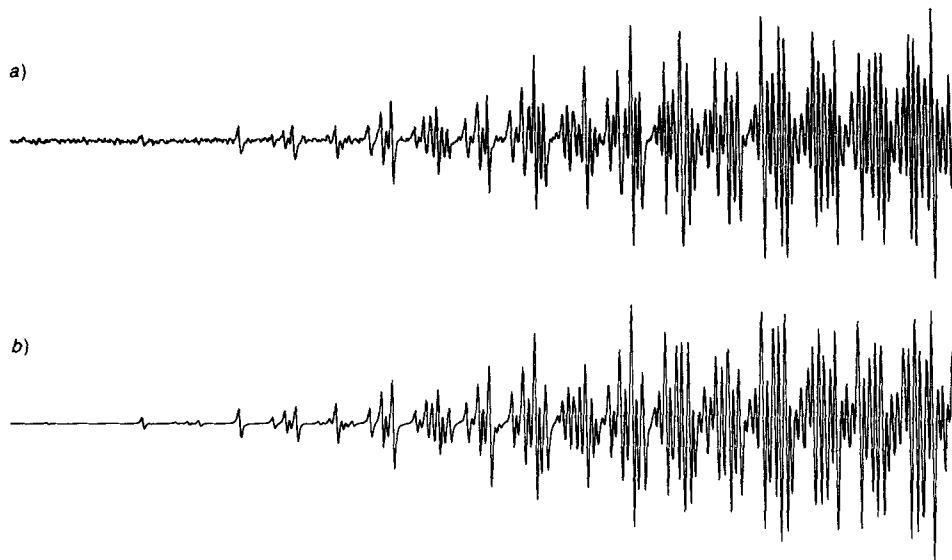


Fig. 2. a) Experimental ESR spectrum of radical **4a** in a $2 \cdot 10^{-3}$ M solution of dimer **3a** in toluene at -25° . b) Calculated spectrum for radical **4a**, using the best-fit coupling constants given in Table 2. Both plots are 7 G wide, the total experimental spectrum width is 19.6 G. The first peak, as well as peaks 3–7, barely visible in the calculated spectrum, are lost in the noise in the experimental spectrum. These peaks can be seen at higher temperatures where the radical concentration is higher, but under these conditions, the resolution is severely degraded by spin exchange.

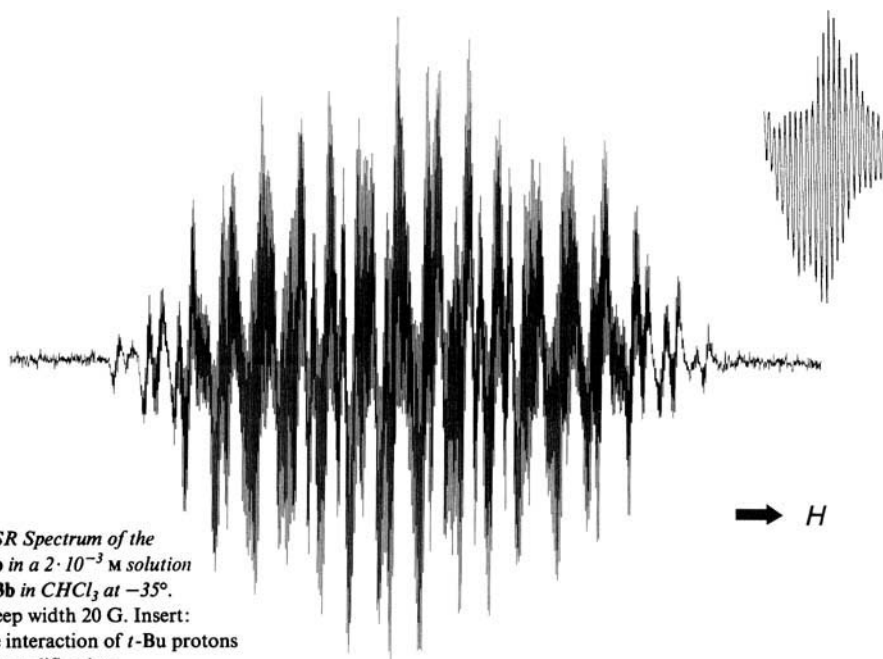
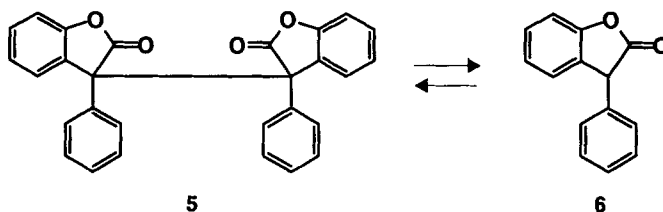


Fig. 3. ESR Spectrum of the radical **4b** in a $2 \cdot 10^{-3}$ M solution of dimer **3b** in CHCl_3 at -35° . Total sweep width 20 G. Insert: hyperfine interaction of *t*-Bu protons at higher amplification.

corresponding best-fit calculated spectrum. Fig. 3 shows the spectrum of radical **4b** at -35° in CHCl_3 ; the 9 equivalent protons of the *t*-Bu group of **4b** have a coupling constant of only 0.045 G. This coupling is well resolved and leads to a highly congested spectrum.

The coupling constants of **4a** were assigned with the help of known coupling constants from a similar system, the oxobenzofuranyl radical **6** [6] (Scheme 2). The best-possible fit

Scheme 2



to the experimental spectrum of **4a**, obtained by computer calculation using various possible combinations of coupling constants, allowed the assignments. From the relative intensities of the first several ESR lines in Fig. 2, the coupling constants at 0.71, 1.05, and 1.13 G could be assigned to the 6 equivalent *ortho*-Me protons, the 2 equivalent *meta*-protons, and the 3 equivalent *para*-Me protons, respectively. By elimination, the two remaining coupling constants near 1.0 G with a statistical weight that corresponds to single protons, must be due to the protons at the 4 and 6 positions. However, it is not possible from the ESR or ENDOR data to differentiate between these two positions. The best-fit coupling constants are given in Table 2. It should be pointed out that the coupling

Table 2. Best-Fit Coupling Constants for Radical **4a**^{a)}

| Proton ^{b)} | H-C(4) ^{d)} | H-C(5) ^{d)} | H-C(6) ^{d)} | H-C(7) ^{d)} | <i>ortho</i> -Me ^{f)} | <i>meta</i> -H ^{f)} | <i>para</i> -Me ^{f)} |
|--------------------------------------|---------------------------|----------------------|--------------------------|----------------------|--------------------------------|------------------------------|-------------------------------|
| Coupling constants [G] ^{c)} | 0.963 (1 H) ^{e)} | 4.20 (1 H) | 1.08 (1 H) ^{e)} | 3.42 (1 H) | 0.713 (6 H) | 1.05 (2 H) | 1.13 (3 H) |

^{a)} Coupling constants giving the best-fit calculated spectrum to the experimental spectrum in toluene at -25° ; calculated and experimental line-widths are 0.016 G peak-to-peak.

^{b)} See Scheme 1 for numbering.

^{c)} ± 0.03 G.

^{d)} Assigned by analysis of the ENDOR and ESR spectra and by analogy with coupling constants in [6].

^{e)} Assignment ambiguous, these two coupling constants could be interchanged; it is not entirely obvious which proton H-C(4) or H-C(6), should have the larger coupling constant.

^{f)} Assigned from the relative ESR-line intensities, see text.

constants of the *ortho*- and *para*-Me protons in **4a** (0.71 and 1.13 G) greatly differ from those expected by comparison with the corresponding values for **6** (2.51 and 2.74 G). Because the coupling constants of β -protons in Me substituents usually have similar absolute values as those of α -protons in these positions, the striking differences in the hyperfine data for **4a** and **6** are diagnostic of the pertinent ring in **4a** being twisted out of planarity with the remaining π -system (see, e.g. [7]).

The 2-chloronaphthalene solution of the higher-melting diastereoisomer of dimer **3c** showed ESR resonances only above 180°. No attempt was made to fully analyze the coupling parameters. No radicals could be observed up to 200° for the diastereoisomer mixture **3d** in 2-chloronaphthalene.

3. *Thermochemistry.* ΔG , ΔH , and ΔS for the homolytic cleavage of the dimers **3a–d** to **4a–d** (see *Scheme 1*) were calculated from the relationship $\ln K = -\Delta G/RT = \Delta S/R - \Delta H/RT$, where K is the equilibrium constant for the homolysis and R the gas constant. A plot of $\ln K$ as a function of the inverse temperature T^{-1} then yields a straight line with an intercept equal to $\Delta S/R$ and a slope of $-\Delta H/R$. To calculate the equilibrium constant at each temperature, it is necessary to know the absolute radical concentration and the dimer concentration. Absolute radical concentrations are notoriously difficult to measure by ESR methods, but at temperatures where the extent of dissociation of the dimer is small, the relation given above simplifies to $\ln[R\cdot]^2 = C - \Delta H/RT$ where $[R\cdot]$ is the radical concentration, and C is an arbitrary constant. The second integral of the ESR signal is proportional to the radical concentration; thus, $\ln[R\cdot]^2$ can be plotted *vs.* T^{-1} without determination of the absolute radical concentration [8]. This gives straight lines with a slope of $-\Delta H/RT$ for radical **4a** in toluene and 2-chloronaphthalene (see *Fig. 4*). To

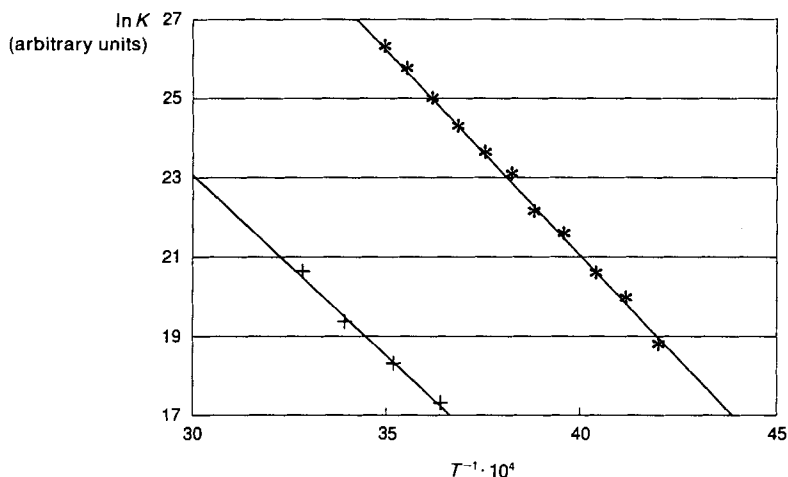


Fig. 4. Plot of the logarithm of the squares of the ESR second integral intensity (arbitrary units) vs. the inverse temperature T^{-1} (in K^{-1}) for solutions of dimer **3a** in toluene (*) and 2-chloronaphthalene (+). Concentration of dimer ca. $4.5 \cdot 10^{-2}$ M. The slopes of the lines are equal to $\Delta H/R$ (see text).

determine the equilibrium constant and ΔG , the absolute radical concentration at several temperatures was measured by comparison with the second integral of the ESR signal from a stable nitroxyl-radical sample of known concentration. ΔS was then calculated from the expression $\Delta S = (\Delta H - \Delta G)/T$. For radical **4c**, an estimate of the equilibrium constant at 190° was made from which an estimate of ΔG was calculated (see *Table 3*). A rough estimate for a lower limit for the bond energy in the dimer **3d** was made using the fact that the equilibrium constant for the homolysis must be less than $1 \cdot 10^{-6}$ M at 200°, since no radicals could be observed in a solution of **3d** in 2-chloronaphthalene at this

Table 3. *Thermodynamic Data for the Homolytic Cleavage of Dimers 3a^a, 3c^b, and 3d^c*

| Dimer | Solvent | ΔH [kcal/mol] | ΔS [Gibbs] | ΔG_{298} [kcal/mol] |
|-----------|-----------------------------------|-----------------------|--------------------|-----------------------------|
| 3a | toluene | 20 ± 1 | 45 ± 5 | 6.5 ± 1 |
| | 2-chloronaphthalene | 16 ± 1 | 40 ± 5 | 5.3 ± 1 |
| 3c | 2-chloronaphthalene ^{d)} | ca. 30 | 40 ^{e)} | ca. 18 |
| 3d | 2-chloronaphthalene ^{f)} | > 30 | 40 ^{e)} | > 18 |

a) Presumably *meso/rac*-**3a** 1:1.

b) Higher-melting diastereoisomer.

c) *meso/rac*-**3d** 1:1.

d) Values for dimer **3c** are estimated from the radical concentration observed at 190°, see text.

e) Assumed to be near the value for dimer **3a**.

f) Dimer **3d** does not dissociate sufficiently to give an ESR signal below the boiling point of 2-chloronaphthalene.

temperature. Table 3 contains a summary of the thermochemical results for the homolysis of the dimers **3a**, **c**, **d**.

4. *Kinetics*. As mentioned above, the best resolution in the ESR spectrum of radical **4a** is obtained with solutions containing low dimer concentration, and at low temperatures. At higher temperatures, the increasing radical concentration leads to more frequent collisions between radicals, and spectra become lifetime-broadened due to spin exchange and recombination reactions. The relationship between the mean lifetime of the radical and the ESR line-width is given by the equation $\Gamma = \Gamma_0 + 1/2 \tau \gamma_e$ where Γ_0 is the line-width in the absence of lifetime broadening, 2τ is the mean lifetime of the radical, and γ_e is the gyromagnetic ratio of the electron [9]. Γ_0 was determined from the line-width of the

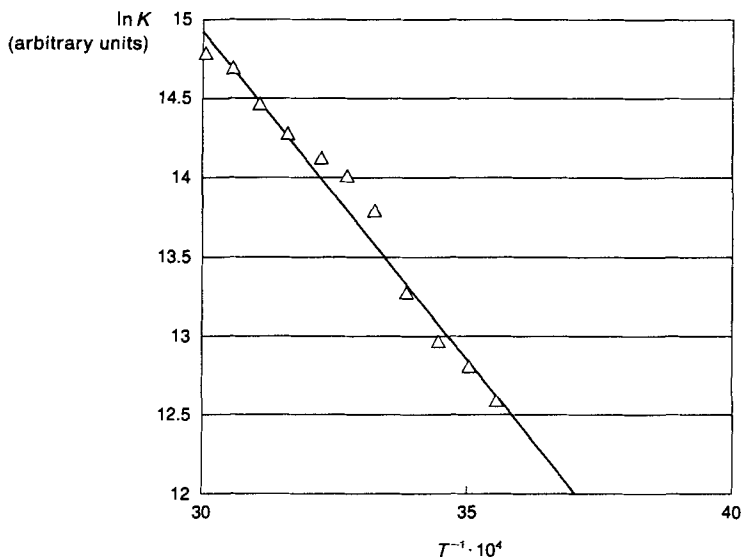


Fig. 5. Plot of the logarithm of the rate constant for line broadening ($k = 1/2\tau$; calculated as described in the text from the ESR line-widths) vs. the inverse temperature T^{-1} (in K^{-1}) for a $2.5 \cdot 10^{-4}$ M solution of dimer **3a** in toluene. The slope of the plot gives the activation energy for spin exchange and radical recombination.

ESR signal of radical **4a** below -30° to be 17.0 mG. The rate constant for line broadening ($k = 1/2\tau$) was obtained at a series of temperatures, and from a plot of $\ln k$ vs. T^{-1} (see *Fig. 5*), the activation energy for the broadening process was determined to be 8.4 ± 2 kcal/mol in toluene. It should be noted that contributions to the lifetime broadening due to both spin exchange and recombination reactions cannot be distinguished by our experiments. The activation energy of 8.4 kcal/mol points to an important contribution of the recombination reaction. The second-order rate constant calculated from the pseudo-first-order rate constant for the bimolecular line broadening (see *Fig. 5*) and from the equilibrium constant is $9 \cdot 10^9 \text{ M}^{-1}\text{s}^{-1}$. This value represents a diffusion-controlled reaction. It is likely that the recombination reaction of radicals **4a** and **4b** to re-form the dimers also proceeds at the diffusion limit. Examples are known [10] where spin exchange occurs at a more rapid rate than recombination.

Discussion. – The radicals **4a, b** are extremely stable in the absence of O_2 . At room temperature in 2-chloronaphthalene, dimer **3a** is dissociated to *ca.* 0.5% to radicals. A $4.5 \cdot 10^{-2} \text{ M}$ solution of **3a** could be cycled repeatedly to 160° in 2-chloronaphthalene, where the dimer is dissociated to 85% to radicals, with no measurable change in the radical concentrations from cycle to cycle. Hence, there are no significant side reactions that deplete the radicals or affect the equilibrium measurements. That the low bond energy in dimers **3a, b** is due largely to relief of steric hindrance upon dissociation can be seen by comparing the thermochemical data of **3a** with those of **3c** and **3d**. Removing one of the *o*-Me groups as in dimer **3c** increases ΔH substantially (see *Table 3*). Removal of both *o*-Me groups results in an increase in the bond energy so great that ESR signals from the radical **4d** could not be observed below 200° in this study. It is interesting to compare these results with previously published [6] results for dimer **5** (*Scheme 2*): ESR signals of the corresponding radical **6** were observed above 70° in xylene. The lower free energy for bond homolysis in dimer **5** compared with **3d** is probably due to a combination of increased steric hindrance from the carbonyl group in α -position to the bond to be broken, as well as increased stabilisation of the resulting radicals by the α -carbonyl group. In dimers **3a** and **3b**, the *o*-Me groups replace the α -carbonyl groups of dimer **5** in providing the steric driving force for bond homolysis.

The lower bond energy measured for dimer **3a** in 2-chloronaphthalene (16 kcal/mol) as compared to the bond energy in toluene (20 kcal/mol) shows that the radical is stabilised by the more polar 2-chloronaphthalene solvent. Such a stabilisation of the radical species by a more polar solvent was reported for a number of nonstable dimers [11]. According to molecular-orbital calculations, radical centers substituted by both electron-donor and electron-acceptor substituents (as radicals **4a–d** and **6**) should exhibit especially high stability (merostabilisation) [12], and the stability should strongly increase with the dielectric constant of the solvent. If a stabilisation by charge-separated resonance structures, also known as capto-dative effect (see review in [13]), was important for radical **4a**, the values of the coupling constants would be expected to vary as the polarity of the solvents is changed [14]. However, ENDOR hyperfine coupling constants of radical **4a** in toluene, 2-chloronaphthalene, and EtOH (see *Table 1*) do not show the expected dependence on the solvent. Since this effect is not observed, it seems likely that the lower bond energy for dimer **3a** observed in 2-chloronaphthalene must be due to some other favourable interaction of this solvent with radicals **4a**, and not due to stabilisation

of charge-separated resonance structures. This is in agreement with investigations by R uchardt and coworkers [15] who came to the conclusion that for each radical solvent pair, the individual structures and interactions have to be considered.

We would like to thank Prof. Dr. F. Gerson for valuable discussions and suggestions. We are also indebted to Prof. Dr. F. Gerson, Dr. T. Wellauer, and Dr. P. Felder at the Department of Physical Chemistry of the University of Basel for the use of their ENDOR spectrometer.

Experimental Part

1. *General.* All reactions were carried out under N₂. Solvents (*Fluka, puriss.*) were dried over molecular sieves before use. All reagents (*purum*) were purchased from *Fluka*. HPLC: *Spectra Physics SP8100 XR* equipped with an *SP-4200* computing integrator and *SP8773-XR* UV detector, $\lambda = 230$ nm; flow 1 ml/min, MeOH/H₂O 4:1 isocratical; column (125 × 4.6 mm), 5- μ m RP-18. M.p.: *Reichert-Austria* hot-plate microscope; uncorrected. IR: *Nicolet 20 SX*. NMR: *Bruker AC 300* (¹H and ¹³C) and *Varian VXR-400 S* (¹H); TMS as internal standard, δ in ppm, J in Hz. EI-MS (70 eV): *Hewlett-Packard HP 5988 A*; in m/z (rel. %).

2. *ESR and ENDOR Spectra.* ESR Spectra: *Varian-E-9-ESR* spectrometer with a variable-temp. accessory and a dual sample cavity. The dimers **3a**, **b**, **d** were used as their *meso/rac* mixtures; in the case of **3c**, the pure higher-melting diastereoisomer was used for measurements. The radicals **4a** and **4b** reacted rapidly with air in soln. To avoid this reactions with O₂ and to improve the resolution in the ESR spectra, the solns. were prepared by dissolving the degassed solid sample in the previously degassed solvent by vacuum transfer of solvent. The solns. sealed in quartz tubes were stable over a period of several months. The spectra were acquired by computer, and the relative radical concentrations at each temp. were obtained by computerised double integration of the digitised spectra. The signal from a solid sample of DPPH (= 2,2-bis(1-picrylhydrazyl)) in the second sample position of the cavity was used to correct for variations in cavity Q . To obtain the absolute radical concentrations, the second integrals from the radicals of interest were compared with second integrals from samples containing known concentrations of the stable free radical 4-(benzoyloxy)-2,2,6,6-tetramethylpiperidin-1-oxyl [16]. The variation in the ESR-integral intensity of the stable free radicals was accounted for on construction of calibration curves over the entire temp. range studied, as described by *Ingold* and coworkers [17]. Several spectra were taken at each temp. and the average of the integrals was used to increase the confidence level of the integral values. The temp. in the sample region was calibrated before and after each experiment using a chromel-alumel thermocouple in an ESR sample tube with solvent. ENDOR Spectra: *Bruker-ESP-300* system with a variable temp. accessory.

3. *2-Aroylbenzoic Acids (1).* The acids **1a**, **1c** [18], and **1d** [19] were prepared according to the described procedures.

3.1. *2-[4-(tert-Butyl)-2,6-dimethylbenzoyl]benzoic Acid (1b).* Powdered phthalic anhydride (49.35 g, 0.33 mol) was added to a suspension of finely powdered AlCl₃ (88.8 g, 0.67 mol) in 1,2-dichloroethane (200 ml) and the mixture stirred 0.5 h at r.t. After cooling to –30°, 1-(*tert*-butyl)-3,5-dimethylbenzene (54.0 g, 0.33 mol) was added dropwise and the temp. allowed to rise to r.t. within 6 h. The mixture was then poured on 1000 g of crushed ice and extracted with several 1-l portions of CH₂Cl₂. The combined extract was washed with H₂O, dried (Na₂SO₄), and evaporated and the residue recrystallised (2 ×) from MeCN: 58.5 g (57%) of **1b**. M.p. 186–189°. IR (KBr): 2960s, 1730s, 1700s, 1670s, 1600m, 1575m, 1480w, 1445w, 1410m, 1360w, 1265s, 1170w, 1135w, 1445w, 940s, 900m, 870m. ¹H-NMR (300 MHz, (D₆)DMSO): 1.30 (s, *t*-Bu); 2.11 (s, 2 Me); 7.14 (s, 2 arom. H); 7.26 (*d*, $J = 7.7$, 1 arom. H); 7.50–7.57 (*m*, 1 arom. H); 7.66 (s, 1 arom. H); 7.67 (s, 1 arom. H); 13.10 (s, COOH). Anal. calc. for C₂₀H₂₂O₃ (310.39): C 77.39, H 7.14; found: C 77.23, H 7.05.

4. *General Procedure for 2a–c.* At r.t., 30 mmol of **I** were stirred with SOCl₂ (10 ml) and DMF (2 drops) for 20 h. Excess SOCl₂ was then evaporated, and the solid residue recrystallised from petroleum ether (80–110°) and dried *in vacuo* over P₂O₁₀.

3-Chloro-3-(2,4,6-trimethylphenyl)isobenzofuran-1(3H)-one (**2a**): Yield 7.8 g (91%). Colourless needles. M.p. 124–126°. IR (nujol): 2952s, 2924s, 2854s, 1785s, 1749m, 1714w, 1666s, 1608m, 1592m, 1574m, 1462s, 1378m, 1297m, 1278m, 1267s, 1197s, 1180m, 1144w, 1100w, 1041w, 956m. ¹H-NMR (300 MHz, CDCl₃): 2.14 (s, 2 Me); 2.34 (s, Me); 6.91 (s, 2 arom. H); 7.40 (*d*, $J = 7.7$, 1 arom. H); 7.47–7.54 (*m*, 1 arom. H); 7.63–7.68 (*m*, 2 arom. H). Anal. calc. for C₁₇H₁₅ClO₂ (286.76): C 71.21, H 5.27, Cl 12.36; found: C 71.07, H 5.10, Cl 12.36.

3-[4-(*tert*-Butyl)-2,6-dimethylphenyl]-3-chloroisobenzofuran-1(3H)-one (**2b**): Yield 9.0 g (91%). Colourless needles. M.p. 126–129°. IR (nujol): 2952s, 2924s, 2854s, 1804s, 1793s, 1705w, 1671s, 1605w, 1593w, 1572m, 1478m, 1461s, 1408w, 1377m, 1362m, 1299w, 1278s, 1268s, 1229w, 1191m, 1169m, 1124w, 1093w, 945s. ¹H-NMR (300 MHz, CDCl₃): 1.33 (s, *t*-Bu); 2.18 (s, 2 Me); 7.09 (s, 2 arom. H); 7.42 (d, *J* = 7.8, 1 arom. H); 7.46–7.53 (m, 1 arom. H); 7.59–7.66 (m, 2 arom. H). Anal. calc. for C₂₀H₂₁ClO₂ (328.84): C 73.05, H 6.44, Cl 10.78; found: C 73.07, H 6.45, Cl 10.85.

3-Chloro-3-(2,5-dimethylphenyl)isobenzofuran-1(3H)-one (**2c**): Yield 7.1 g (87%). Colourless needles. M.p. 107–109°. IR (nujol): 2953s, 2924s, 2854s, 1789s, 1749m, 1680w, 1609w, 1600m, 1499m, 1466s, 1377m, 1338w, 1284s, 1267s, 1232s, 1193w, 1162m, 1128w, 1099m, 1071s, 1044w, 1021m, 1008s, 974s. ¹H-NMR (300 MHz, CDCl₃): 2.27 (s, Me); 2.58 (s, Me); 7.12 (d, *J* = 7.7, 1 arom. H); 7.18 (d, *J* = 7.7, 1 arom. H); 7.26 (s, 1 arom. H); 7.66 (dd, *J* = 7.2, 7.7, 1 arom. H); 7.76 (d, *J* = 7.7, 1 arom. H); 7.85 (dd, *J* = 7.2, 7.7, 1 arom. H); 7.95 (d, *J* = 7.7, 1 arom. H). Anal. calc. for C₁₆H₁₃ClO₂ (272.73): C 70.46, H 4.80, Cl 13.00; found: C 70.42, H 4.74, Cl 12.77.

The known [20] oily **2d** was prepared according to the above general procedure and used after evaporation of SOCl₂ without further purification for the synthesis of **3d**.

5. *General Procedure for 3a–d*. At 40°, **2** (5 mmol) was dissolved under N₂ in carefully N₂-purged acetone (10 ml). To the stirred soln. was added by syringe 1M NaI in acetone (7.5 ml). The mixture was stirred 1 h at r.t. and then 0.5M Na₂S₂O₅ in N₂-purged H₂O (20 ml) added. The precipitate of **3** was filtered off, washed with N₂-purged H₂O, and dried over P₄O₁₀ *in vacuo*.

meso/rac-1,1'-Bis(2,4,6-trimethylphenyl)-1,1'-bi(isobenzofuran)-3,3'-(1H,1'H)-dione (**3a**): Yield 1.01 g (80%). White, microcrystalline powder. M.p. 125–135° (red colour of the melt). IR (KBr): 2971w, 2923w, 1780s, 1611m, 1596w, 1480w, 1466m, 1457w, 1379w, 1286m, 1263m, 1242m, 1107m, 1090w, 1075w, 1034w, 1019w, 992m. ¹H-NMR (400 MHz, CDCl₃, –60°; only one diastereoisomer visible): 2.10 (s, Me); 2.21 (s, Me); 2.37 (s, Me); 6.70 (s, 1 arom. H); 6.73 (s, 1 arom. H); 7.48 (dd, *J* ≈ 8.0, 8.0, 1 arom. H); 7.54 (d, *J* = 8.0, 1 arom. H); 7.72 (dd, *J* ≈ 8.0, 8.0, 1 arom. H); 7.86 (d, *J* = 8.0, 1 arom. H). MS: 252 (17), 251 (100), 222 (11.4), 209 (5.9), 208 (36.4), 193 (5), 180 (9), 179 (12.5), 178 (13.6), 165 (16.5). Anal. calc. for C₃₄H₃₀O₄ (502.61): C 81.25, H 6.02; found: C 81.12, H 6.07.

meso/rac-1,1'-Bis[4-(*tert*-butyl)-2,6-dimethylphenyl]-1,1'-bi(isobenzofuran)-3,3'-(1H,1'H)-dione (**3b**): Yield 1.07 g (73%). White, microcrystalline powder. M.p. 118–135° (red colour of the melt). IR (KBr): 2964s, 2903m, 2868m, 1783s, 1731m, 1673m, 1604m, 1575w, 1561w, 1482m, 1466s, 1423w, 1407w, 1394w, 1380w, 1363m, 1335w, 1286s, 1263s, 1244s, 1231s. ¹H-NMR (400 MHz, CDCl₃, –60°; only one diastereoisomer visible): 1.22 (s, *t*-Bu); 2.14 (s, Me); 2.24 (s, Me); 6.69 (d, *J* = 2.0, 1 arom. H); 6.86 (d, *J* = 2.0, 1 arom. H); 7.49 (dd, *J* ≈ 8.0, 8.0, 1 arom. H); 7.57 (d, *J* = 8.0, 1 arom. H); 7.74 (dd, *J* ≈ 8.0, 8.0, 1 arom. H); 7.91 (d, *J* = 8.0, 1 arom. H). MS: 586 (3), 310 (8.4), 309 (30.9), 308 (8.5), 295 (5.7), 294 (30), 293 (100), 292 (9), 291 (11). Anal. calc. for C₄₀H₄₂O₄ (586.77): C 81.88, H 7.22; found: C 81.70, H 7.26.

meso/rac-1,1'-Bis(2,5-dimethylphenyl)-1,1'-bi(isobenzofuran)-3,3'-(1H,1'H)-dione (**3c**): Yield 0.90 g (76%). White, microcrystalline powder. M.p. 195–215°. Chromatography (silica gel, CH₂Cl₂) of 0.8 g of this material afforded 0.38 g of the diastereoisomer melting at 206–209° and 0.32 g of the more polar diastereoisomer melting at 224–226°.

Lower-Melting Diastereoisomer of 3c: White, microcrystalline powder. IR (KBr): 2969w, 2924w, 2872w, 1776s, 1608w, 1595w, 1500w, 1466m, 1447w, 1285m, 1244m, 1218w, 1167w, 1105m, 1091m, 1074m, 1039w, 1015w, 1105m, 1091m, 1074m, 1039w, 1015w, 980m, 965m. ¹H-NMR (300 MHz, CDCl₃): 2.02 (s, Me); 2.18 (s, Me); 6.91 (s, 2 arom. H); 7.26–7.32 (m, 1 arom. H); 7.47–7.59 (m, 3 arom. H); 7.78 (s, 1 arom. H). MS: 238 (18), 237 (100), 194 (6.5), 166 (10), 165 (19). Anal. calc. for C₃₂H₂₆O₄ (474.56): C 80.99, H 5.52; found: C 80.88, H 5.54.

Higher-Melting Diastereoisomer of 3c: White, microcrystalline powder. IR (KBr): 2977w, 2937w, 2868w, 1775s, 1612w, 1592w, 1498w, 1466m, 1286m, 1244m, 1234m, 1163w, 1116m, 1076m, 1037s, 991w, 960w. ¹H-NMR (300 MHz, CDCl₃): 2.24 (s, Me); 2.26 (s, Me); 6.87–6.95 (m, 2 arom. H); 7.38 (s, 1 arom. H); 7.47–7.63 (m, 3 arom. H); 7.76 (d, *J* = 7.5, 1 arom. H). MS: 238 (15), 237 (100), 166 (5), 165 (8). Anal. calc. for C₃₂H₂₆O₄ (474.56): C 80.99, H 5.52; found: C 80.68, H 5.54.

meso/rac-1,1'-Bis(4-methylphenyl)-1,1'-bi(isobenzofuran)-3,3'-(1H,1'H)-dione (**3d**): From crude **2d** on a six-fold scale (12 h): 5.4 g (81%) of **3d** as a brown microcrystalline powder. The crude **3d** was not separable on TLC (silica gel, CH₂Cl₂). A good anal. separation was achieved by reversed-phase HPLC: two diastereoisomers in ratio 49.2:48.6. Filtration of 2 g of crude **3d** through a short silica-gel column using CH₂Cl₂ afforded 1.7 g of pure, white **3d** (*meso/rac*). M.p. 225–265°. [21]: M.p. 247–248°. IR (KBr): 3033w, 2922w, 1779s, 1611w, 1595w, 1513w, 1466m, 1287m, 1246m, 1226w, 1193w, 1174w, 1103w, 1074m, 1023m, 1006m, 972w, 808m. ¹H-NMR (300 MHz, CDCl₃): 2.16, 2.25 (2s, 1:1, Me); 6.89–8.34 (m, 8 arom. H). MS: 224 (15), 223 (100), 165 (8) 11. Anal. calc. for C₃₀H₂₂O₄ (446.50): C 80.70, H 4.97; found: C 80.62, H 4.98.

REFERENCES

- [1] See, e.g., F. Ullmann, *Liebigs Ann. Chem.* **1896**, 291, 17; H. Meyer, *Monatsh. Chem.* **1904**, 25, 1177; H. Bauer, G. Endres, *J. Prakt. Chem.* **1913**, 87, 545; A. M. Creighton, L. M. Jackman, *J. Chem. Soc.* **1960**, 3138.
- [2] M. V. Bhatt, K. M. Kamath, M. Ravindranathan, *J. Chem. Soc. (C)* **1971**, 3344.
- [3] M. V. Bhatt, M. Ravindranathan, *J. Chem. Soc., Perkin Trans. 2* **1973**, 1158.
- [4] J.-C. Gramain, M. F. Lhomme, *Bull. Soc. Chim. Fr.* **1981**, 141.
- [5] M. Pfau, F. Gobert, J.-C. Gramain, M.-F. Lhomme, *J. Chem. Soc., Perkin Trans. 1* **1978**, 509.
- [6] P. Karafiloglou, J.-P. Catteau, A. Lablache-Combier, H. Ofenberg, *J. Chem. Soc., Perkin Trans. 2* **1977**, 1545.
- [7] K. Schreiner, A. Berndt, *Angew. Chem. Int. Ed.* **1974**, 13, 144.
- [8] A. Haas, K. Schlosser, S. Steenken, *J. Am. Chem. Soc.* **1979**, 101, 6282.
- [9] M. C. R. Symons, in 'Chemical and Biochemical Aspects of Electron Spin Resonance Spectroscopy', Van Nostrand Reinhold Co., New York, 1978, pp. 103ff.
- [10] See, e.g., S. Tero-Kubota, Y. Sano, Y. Ikegami, *J. Am. Chem. Soc.* **1982**, 104, 3711.
- [11] M. Lazar, J. Rychly, V. Klimo, P. Pelikan, L. Valko, in 'Free Radicals in Chemistry and Biology', CRC Press, Boca Raton, Florida, 1989, pp. 109ff.
- [12] A. R. Katritzky, M. C. Zerner, M. M. Karelson, *J. Am. Chem. Soc.* **1986**, 108, 7213.
- [13] H. G. Viehe, Z. Janousek, R. Merényi, *Acc. Chem. Res.* **1985**, 18, 148.
- [14] See, e.g., the discussion in: J. B. Olson, T. H. Koch, *J. Am. Chem. Soc.* **1985**, 108, 756.
- [15] H. Birkhofer, J. Hädrich, H. D. Beckhaus, Ch. Rüchardt, *Angew. Chem. Int. Ed.* **1987**, 26, 573; H. D. Beckhaus, Ch. Rüchardt, *ibid.* **1987**, 26, 770.
- [16] E. G. Rozantsev, in 'Free Nitroxyl Radicals', Plenum Press, New York-London, 1975, p. 216.
- [17] K. Adamic, J. A. Howard, K. U. Ingold, *Can. J. Chem.* **1969**, 47, 3803.
- [18] G. Baddeley, G. Holt, S. M. Makar, *J. Chem. Soc.* **1952**, 2415.
- [19] *Org. Synth.*, Coll. Vol. I, 2nd edn., pp. 517.
- [20] H. Limpricht, O. Wiegand, *Liebigs Ann. Chem.* **1900**, 311, 178.
- [21] J. O'Brochta, A. Lowy, *J. Am. Chem. Soc.* **1939**, 61, 2765.